Comparison of phase shift cascade and global matrix elastic wavefield modeling

Yanpeng Mi and Gary F. Margrave

ABSTRACT

An analysis of the spectral variation of the surface displacement and velocity fields caused by PP and PS modes in two types of models is presented. According to the generalized O'Doherty-Ansty equation, the high frequency content of seismic transmissivity should be attenuated by multiple scattering which occurs in finely layered media and the attenuation effect is also offset/angle dependent. By using geological models of different number of layers and thickness, we looked for this phenomenon in synthetic data in which interbed multiple reflections are taken into account. The geological models are derived from the well log from Blackfoot 09-08 and the synthetic seismograms are calculated using forward wavefield modeling by phase shift cascade (ELMO) and OSIRIS, a commercial forward modeling software based on the direct global matrix approach. Observation on the synthetic data shows that the effect of multiple scattering on the amplitude spectrum of displacement field is offset dependent. Its variation with the number of layers and the thickness of the layers is also observed. However, we did not observe an obvious attenuation effect over a certain bandwidth.

INTRODUCTION

A major challenging task in seismic methods is accounting for the multiple scattering effect on the frequency content of the seismic data. Such an effect is often caused by stacks of thin sediment layers which are found in many sedimentary basins. Typically such thin sediment layer stacks appear as sand/shale with rather large acoustic impedance contrast. This problem has been addressed by many authors since early 1970's. O'Doherty and Anstey (1971), as a result of mainly heuristic reasoning, provided a formula for the absolute value of the time-harmonic transmissivity that is valid for the whole frequency domain and vertical incidence only. However, their formula does not describe the kinematics of the wavefield, e.g., the phase or group velocity of the transmitted wave. Banik et al. (1985) obtained the same expression for a statistically averaged wavefield. Shapiro et al. (1994, 1996) extended this theory to the case of under-critical oblique incidence for the models compiled by the method of statistical averaging. The formulas they provided described the effect of multiple scattering on kinematics and dynamics of the time-harmonic transmissivity which corresponded to time-harmonic plane waves, and transient transmissivity, which corresponded to a delta pulse as incident wavelet. This theory is useful for correction of the pulse distortion of seismic reflection data from reservoirs for the effect of finely stratified overburdens. This correction may be applied for a reliable analysis of amplitude variation with offset (AVO) (Widmaier et al., 1994).

Contents

OFFSET/ANGLE DEPENDENT MULTIPLE SCATTERING EFFECT

By studying the response in the lower homogeneous half-space to the incident P-wave and SV-wave travelling through a inhomogeneous medium from the upper homogeneous half-space, Shapiro et al. (1996) gave the angle dependent attenuation characteristics of PP and SV-wave transmissivity (figure 1). It can be clearly seen that for P-wave, in the low frequency band, the smaller the incident angle, the larger the attenuation, in the high frequency band this dependence is inverted. There also exist a dramatic angle-dependence for SV wave transmissivity.

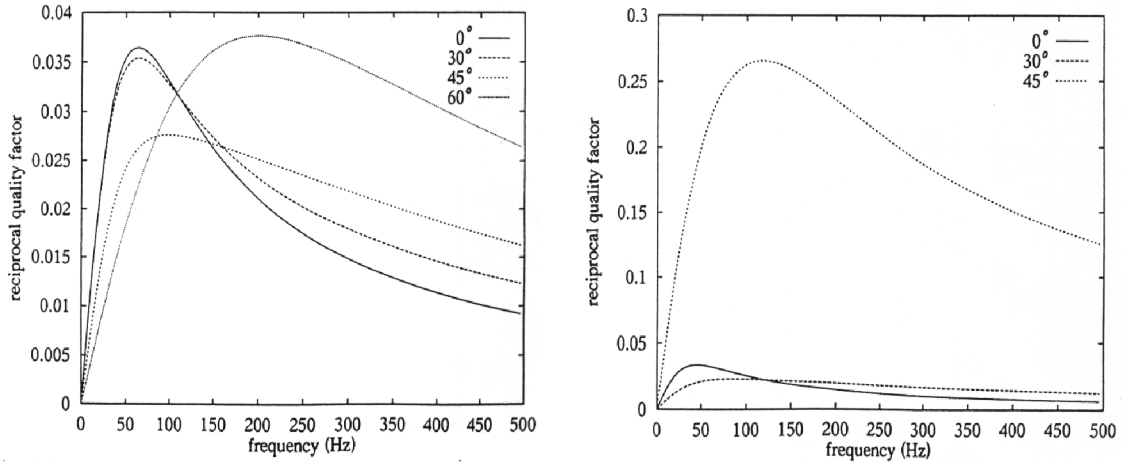

Figure. 1 P and SV wave attenuation coefficient variation with frequency and incident angle [Shapiro, et al., 1996]

The multiple scattering effect variation with the number and thickness of the layers in a model hasn't been discussed sufficiently by former authors. The purpose of this paper is to further examine the offset-dependent multiple scattering effect, as well as its variation with the model complexity. Instead of using the transient transmissivity, we directly examine the amplitude spectrum of the surface displacement and velocity fields of the following cases:

1: Displacement and velocity fields of full wavefields, for a stacks of layers with different complexity.

2: Displacement fields of separated pure P wave and converted SV wave with and without multiple scattering effect, for a realistic geological model.

3: Displacement and velocity fields of the full wavefield at receivers for a P wave point source, for the realistic geological model.

We set up two sets of models and calculated the synthetic data using two forward modeling programs. They are Elastic Wavefield Modeling (ELMO) [Silawongsawat, 1998] and OSIRIS, a commercial software. We also compared the result from these two modeling packages.

MODEL PREPARATION

The geological models are based on the well log Blackfoot 09-08. The log data was collected at the interval of 0.1524 m from 220 m to 1563 m. Figure 2A shows the P, S-wave velocity and density from the well log. Two models were derived from the well log using the log editing tools in Hampson Russell AVO package. The first model is focused on the log from 220 m to 319 m where very fine sediment layers are located. We blocked this zone uniformly into different numbers of layers (25, 57 and 102) in order to study the amplitude spectrum variation with the number of layers and offset. The second model has 24 layers non-uniformly blocked from the whole well log in order to simulate realistic geology (figure 2B). The geometry of the two models is summarized in table I. The synthetic data are calculated using both ELMO and OSIRIS.

Model	Source Type	Received Field	Near Offset	Far Offset	Group Interval	Depth Interval	Number of layers
I	P wave cylindrical pulse	Displacement fields and Velocity fields	0 m	1500 m	5 m	0 – 320 m	25,57,102
II	P wave point source		0 m	2000 m	3.8 m	0-1563m	24

Table. I Two models blocked from the well log Blackfoot 09-08.

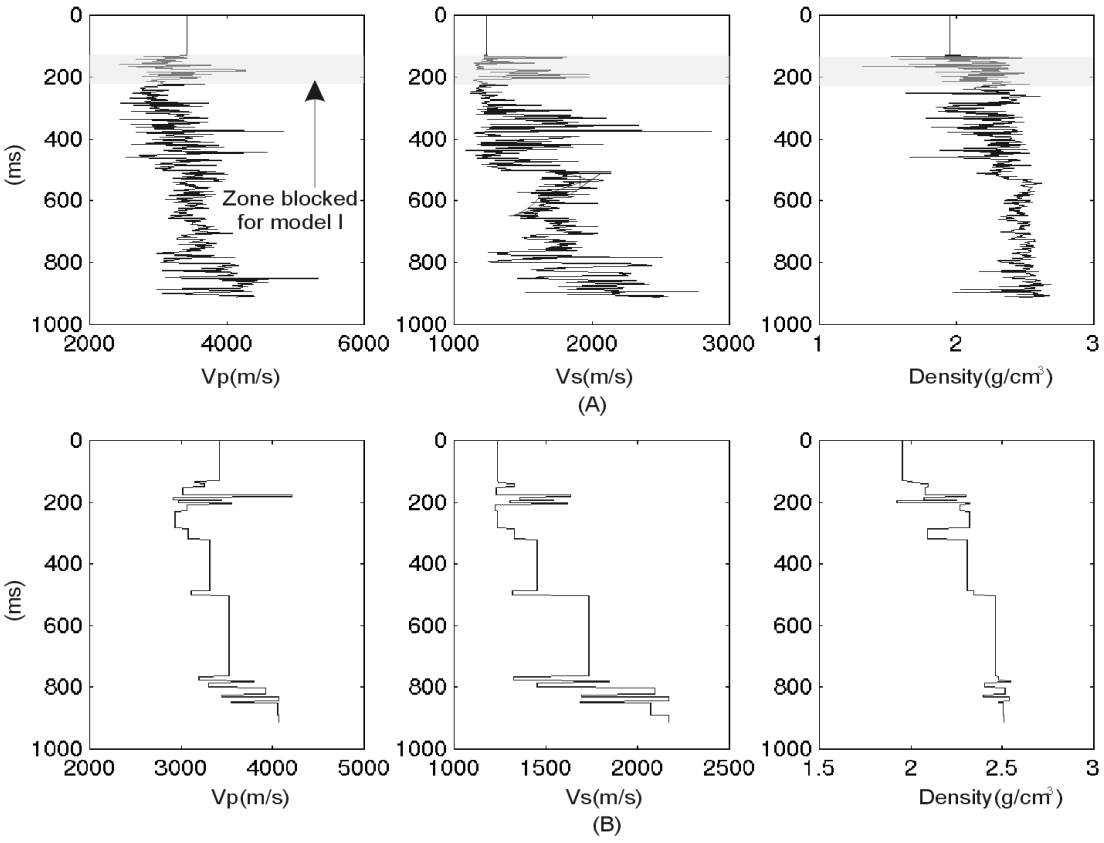

Figure. 2 P, S velocity and density of well log Blackfoot 09-08. (A) Model I is focused on 219 m-319m and is blocked into 25, 57 and 102 layers. (B) Model II is non-uniformly blocked from the whole well log.

Contents

INTRODUCTION TO CALCULATION PROGRAMS

ELMO employs the phase-shift cascade method to calculate the propagating wavefield. Details of theory derivation and algorithm description can be found in Silawongsawat and Margrave (1997). Below we only give a brief introduction to the theory and algorithm.

The history of P and S wave propagation can be written as:

$$\Phi(kx,z,\omega) = \Phi_{dc}(z-\Delta z)e^{ik_z\Delta z} + \Phi_{uc}(z+\Delta z)e^{ik_z\Delta z} \tag{1}$$

$$\Psi(kx,z,\omega) = \Psi_{dc}(z-\Delta z)e^{ik_z\Delta z} + \Psi_{uc}(z+\Delta z)e^{ik_z\Delta z} \tag{2}$$

where Φ and Ψ are P and S wavefield potentials. These two equations can be used to recursively extrapolate each Fourier plane wave from a surface source downward to reflectors and from reflectors upward to the surface. Down-going and up-going P and S wave fields are maintained along the calculation path. The complex amplitude of each wave field at each interface is calculated by using the Zoeppritz reflection and transmission coefficients. The relation between the four outgoing wavefields and four incoming wavefields at an interface can be expressed as:

$$\begin{bmatrix} \Phi_{dg} \\ \Psi_{dg} \\ \Phi_{ug} \\ \Psi_{ug} \end{bmatrix} = \begin{bmatrix} T_{pp} & T_{sp} & \overline{R_{pp}} & \overline{R_{sp}} \\ T_{ps} & T_{ss} & \overline{R_{ps}} & \overline{R_{ss}} \\ R_{pp} & R_{sp} & \overline{T_{pp}} & \overline{T_{sp}} \\ R_{ps} & R_{ss} & \overline{T_{ps}} & \overline{T_{ss}} \end{bmatrix} \begin{bmatrix} \Phi_{dc} \\ \Psi_{dc} \\ \Phi_{uc} \\ \Psi_{uc} \end{bmatrix} \tag{3}$$

where R and T denote reflection and transmission coefficients, subscripts p and s denote mode conversion. Up-going wavefield is specified with a bar over the appropriate values.

Currently ELMO uses a cylindrical P-wave point source at the surface (z=0) without considering the up-going wave above surface. The source can be represented by:

$$S(k_x,\omega) = \frac{i}{k_{z1}} = \frac{i}{\sqrt{\frac{\omega^2}{\alpha_1^2} - k_x^2}} \tag{4}$$

with the boundary condition on P wave field at the surface for a point source:

$$\Phi(kx,0,\omega) = \frac{i}{k_{z1}} W(\omega) e^{i(k_x x - \omega t)} \tag{5}$$

where W is the wavelet term. S wave point source can be easily written in a similar form and implemented in the program [Silawonsawat, 1998]. Two source wavelets, Hanning and Gaussian wavelets, have been implemented in ELMO. The calculation using Hanning wavelet is faster because all the frequency components have to be

Contents

calculated for the Gaussian wavelet. We used the Hanning wavelet in our calculation. Another thing worth to mention is that the free surface effect has not yet been implemented in ELMO.

ELMO is written in the Matlab environment. The source codes of relevant programs in the package are available through the CREWES Project software release. The explicit formulation allows the users to acquire various desired physical results with selective contributions. This is a major advantage of phase-shift cascade over other wave equation based methods.

OSIRIS is commercial forward seismic modeling software developed by ∅degaard A/S. It employs a direct global matrix method [Schmidt and Tango, 1986] for computation of synthetic seismograms in a layered visco-elastic media. The method is suitable for VSP simulation, seismic shot record simulation, transmission loss simulation as well as simulation of vibrating foundations. The global matrix method is based on an integral transform approach, which implies a limitation to horizontal stratified visco-elastic and/or visco-acoustic layers. Attenuation and dispersion effects are included in the method, which makes it applicable to time as well as frequency response simulation with different source types such as point compressional or shear wave sources, point forces and circular surface sources. Details of this method can be found in the final report of "High-Speed Forward Modeling Applied in Seismic Data Processing" from ∅degaard A/S.

To make the data from OSIRIS comparable to that generated with ELMO, a Hanning sine wavelet with dominant frequency of 70 Hz is used to generate the synthetic data and the sample rate is set to 2ms.

DATA ANALYSIS

I. Amplitude spectral variation with the model complexity

By fully engaging all the switches in the scattering matrix in ELMO, we calculated the particle displacement field at the surface receivers as the result of full wave field for model I with different number of layers. The impulse response of the P and S primary and multiples are also calculated. Figure 3 shows the impulse response of the P, SV primaries and primaries with multiple for the 25-layer model. However, when multiples are added, serious artifacts occur for the 57- and 102-layer models. As a consequence, the overall particle displacement response to the full wavefield was not interpretable for the 57- and 102-layer models due to these serious artifacts. We only used the particle displacement response for the P and S primaries. Particle velocity fields at the surface receivers were calculated with OSIRIS. All the P and S primaries, mode conversions and multiples are included in the data. The wavefield separation can be done in OSIRIS but the analysis is numerically unstable.

The vertical displacement fields in the models with different number of layers only show minor differences in the primary arrivals (figure 4A and 4B). Converted SV wave arrivals occur quite close to zero offset in the horizontal displacement field while close to 100m (trace 20) in the vertical displacement field. This near offset difference is due to the SV wave arrival angle at the surface. A general SV wave

Contents

amplitude decreasing with the increment of the number of layers can be observed clearly on both the horizontal and vertical displacement fields. The amplitude of the converted wave near 0.3s get weaker as the number of layer increases. This is probably due to transmission losses.

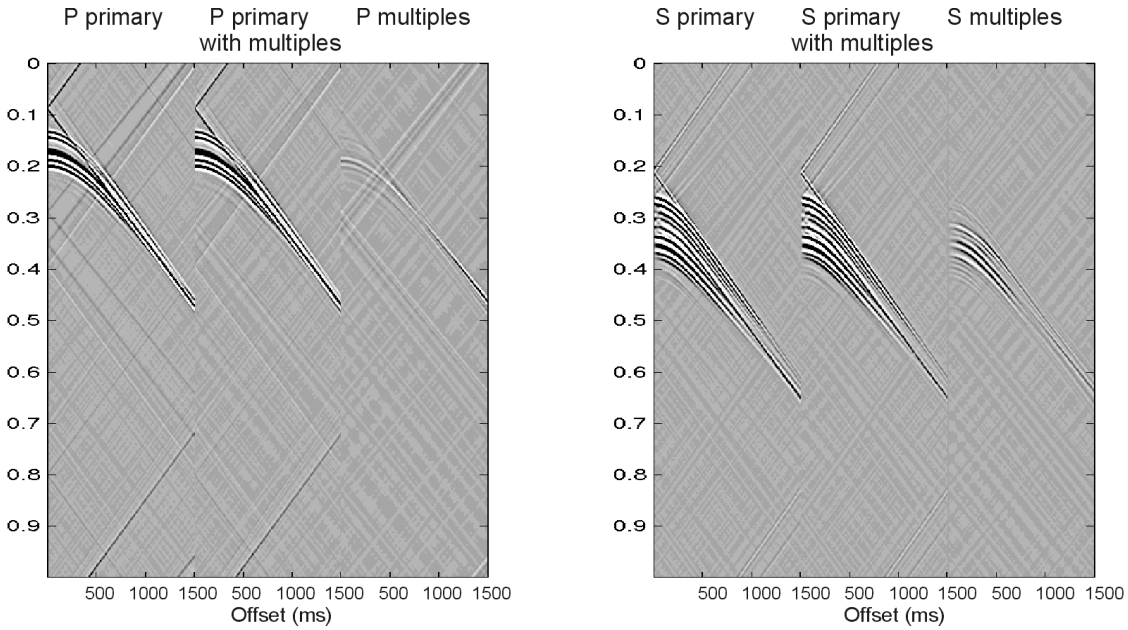

Figure. 3 Impulse response of the P primary, P primary with multiples, S primary and S primary with multiples for the 25-layer model.

The velocity fields calculated with OSIRIS generated the same P and converted SV primary arrivals at 0.13s and around 0.3s, but the full wavefield is much richer. Direct and reflected S wave arrivals are also clearly seen on both the vertical and horizontal velocity fields (figure 4C and 4D) and their amplitude increase as the number of layer increases. Comparing with the data calculated with ELMO, OSIRIS generates strong P and converted SV wave multiples.

We restricted our spectral analysis window from 0.1s to 0.5s so that both the P and SV primaries are included in the window and the artifacts in later arrival times are excluded. Figure 5 shows the displacement and velocity amplitude spectrum variation with the complexity of the models, as well as their variation with offset. Both of the horizontal and vertical displacement amplitudes for the 25-layer model always remain strongest, 57-layer remain medium and the 102-layer model remains weakest. This might due to transmission loss getting larger as the number of layers increases.

The velocity amplitude variation with the complexity of the models is rather ambiguous. The 25-layer model seems to be the weakest one in the horizontal velocity field while rather of the same amplitude with the other two models in the vertical velocity fields. The difference between their amplitudes is minor. However, keep in mind that the data calculated from OSIRIS includes the full wave field effect, i.e., P and S direct and reflected waves, P-SV mode conversions, and interbed

multiples. It is possible that when the thickness of the layers get larger and larger, the interbed multiples may cause some constructive effects.

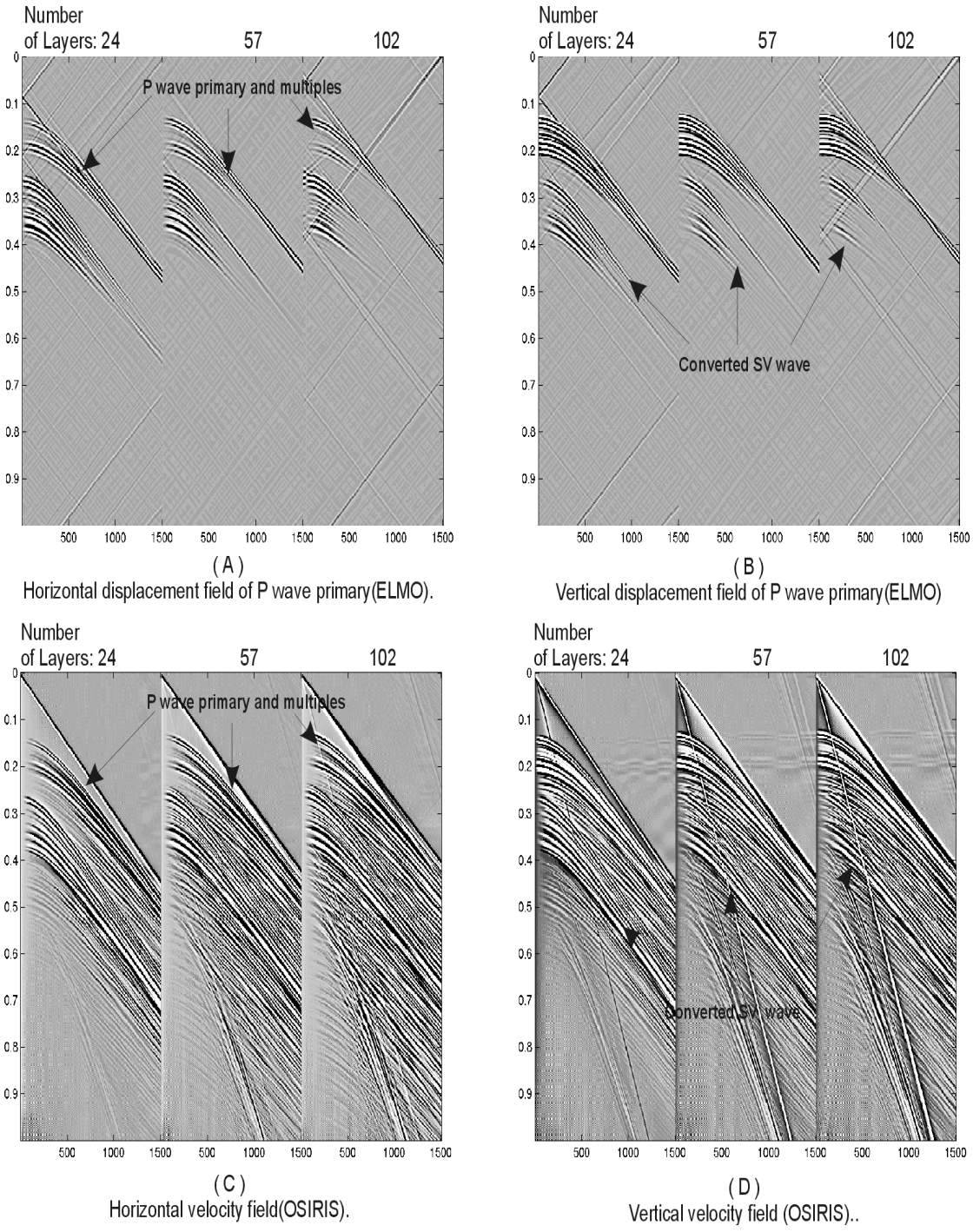

Figure. 4 Displacement and velocity fields of model I. Displacement and velocity fields were calculated with ELMO and OSIRIS, respectively.

Contents

II Amplitude spectral variation with offset.

Figure 5 also shows the displacement and velocity amplitude spectrums at offsets of 250m, 500m and 750m. We can see that both of the horizontal and vertical displacement amplitude decreases with offset. This is probably due to NMO convergence. Note that the difference between the 57- and 102-layer models at the same offset is minimal, which indicates that the transmission loss may not vary much when the thickness of the layers is smaller than a threshold value. The horizontal velocity amplitude increases with the offset from 250 m to 500 m and remains the same level for 500 m and 750 m offset. The same thing happens to the vertical velocity components. Both the displacement and velocity fields for the 57- and 102-layer are at the same amplitude level, which indicates the characteristics of transmission loss has a large change between 25 and 57 layer models.

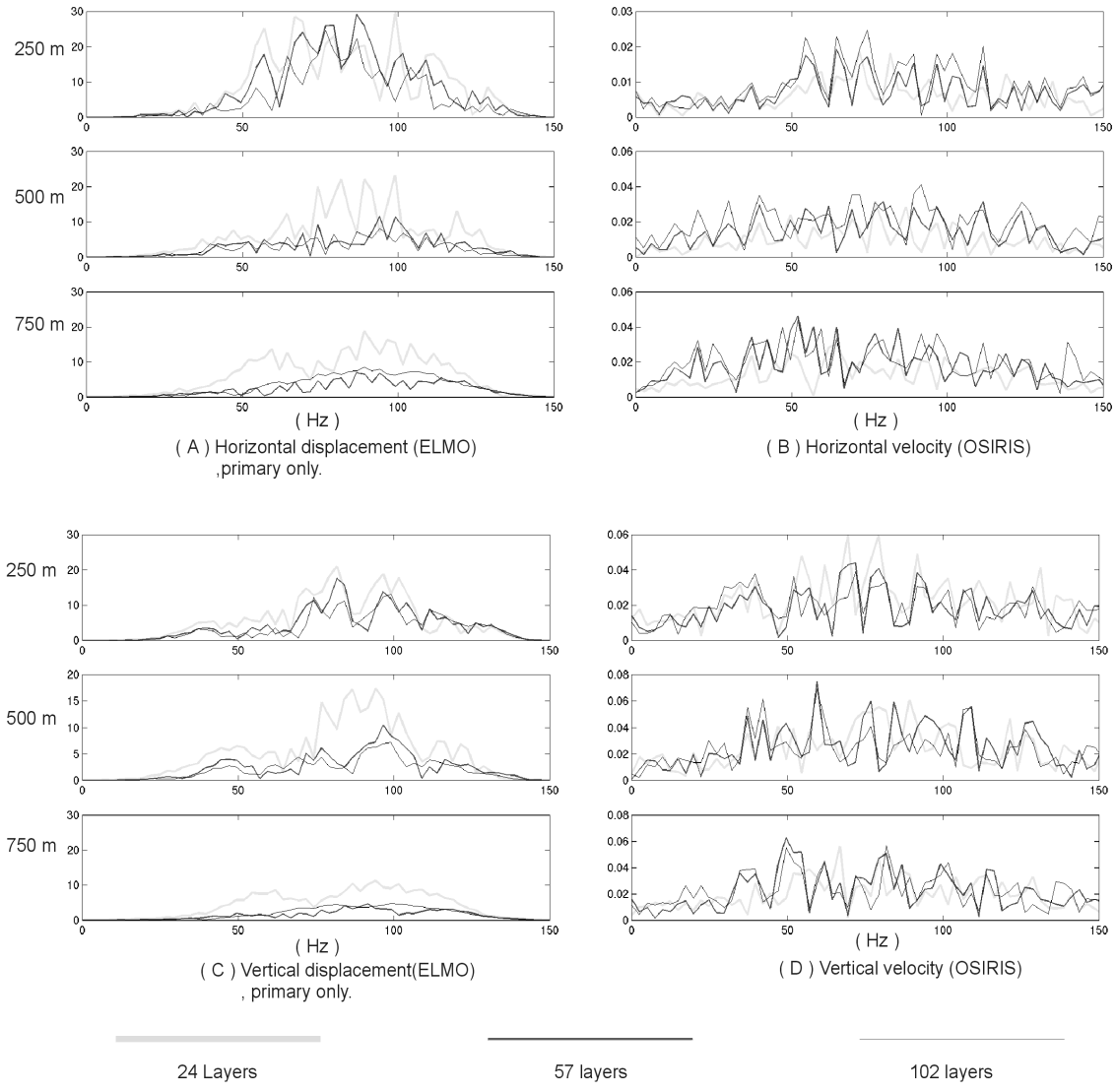

Figure. 5 Displacement and velocity amplitude spectral variation with the complexity of the models. Note that each row in the figures is a different offset.

Contents

III Realistic geological model

For the realistic geological model which was derived by blocking the whole well log into 24 layers based on the lithology variation, we calculated the pure P wave, S wave and P and converted SV wave particle displacement at the surface receivers using ELMO. Velocity fields are also calculated using OSIRIS.

In the synthetic data calculated from ELMO, we can now further examine the amplitude spectral variation versus offset for pure P and S waves, as well as the full wavefield response including converted SV waves. Note that "pure P" wave in ELMO is the P wave at the receiver which contains many mode conversions and this is similar for "pure S". Figure 6 shows the horizontal and vertical displacement fields for pure P wave primary and primary with multiples. Similar to the analysis done on model I, we also calculated the spectral variation with offset. We can see that the near offset horizontal displacement is rather weak compared with that at middle offset at 500m. The middle offset trace has maximum amplitude above 80 Hz. This is mainly due to the P wave arrival angle at the surface. The amplitude of vertical displacement field for pure P waves reduces as the offset gets larger. The addition of multiples causes a lot of notches in their amplitude spectrum but does not give obvious attenuation within a certain bandwidth. Compared with the notches caused by reflections, these notches are deeper. Perhaps multiple effect can be removed by identifying and removing these deep notches.

The displacement fields for the S wave primaries have large variation versus offset but there is no sign of attenuation in a certain bandwidth, either (figure 7). The amplitude spectrum of S primary is only a smoothed version of the S primary with multiples. However, we are able to see that the S wave multiples is dominant in the time section.

In the "pure S" data from ELMO, both the horizontal and vertical displacement fields decay much faster than those in the "pure P" data. This indicates that the data contains more P wave components than S wave components at far offset.

The velocity fields generated with OSIRIS are rather comparable in terms of P and converted SV wave primaries. However, OSIRIS generated much stronger multiples, as we can see from figure 8.

COMPARISON OF ELMO AND OSIRIS

There are several differences between ELMO and OSIRIS in terms of forwarding modeling approach method, numerical stability and calculation speed.

ELMO computes reflections, transmissions and conversions at each interface using modified-for-potential Zoeppritz equations. All the four incident waves are used to generate the four resultant waves for a full solution. ELMO is rather flexible in generating desired wavefields by simply including or excluding some physical effects with a properly reformed scattering matrix. ELMO is designed for simple horizontal layering and not for complex structures. Currently ELMO has only a P wave source and can only do a surface receiver spread.

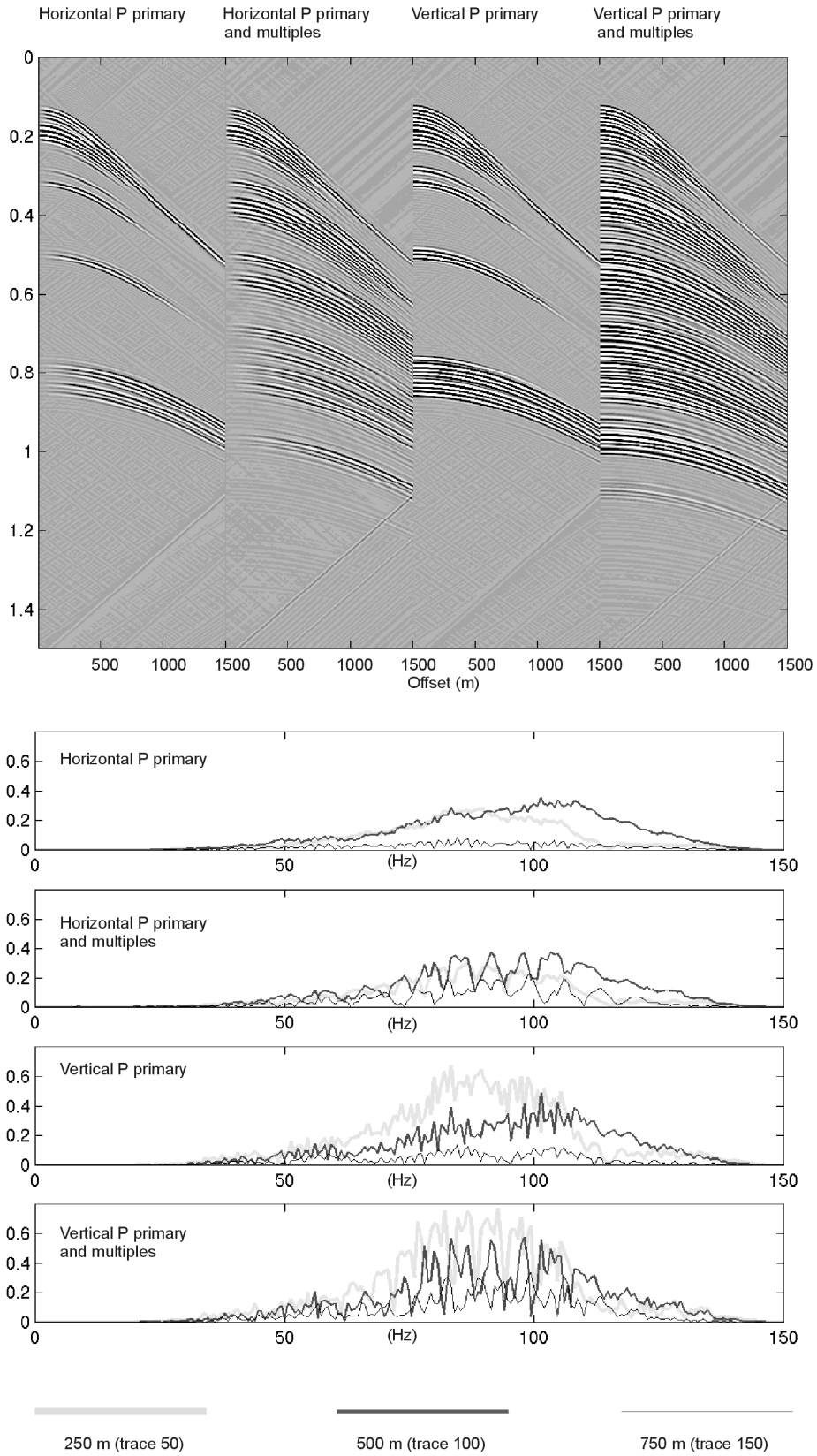

Figure. 6 The displacement fields and their amplitude spectral variation with offset for model II for pure P waves from ELMO.

Contents

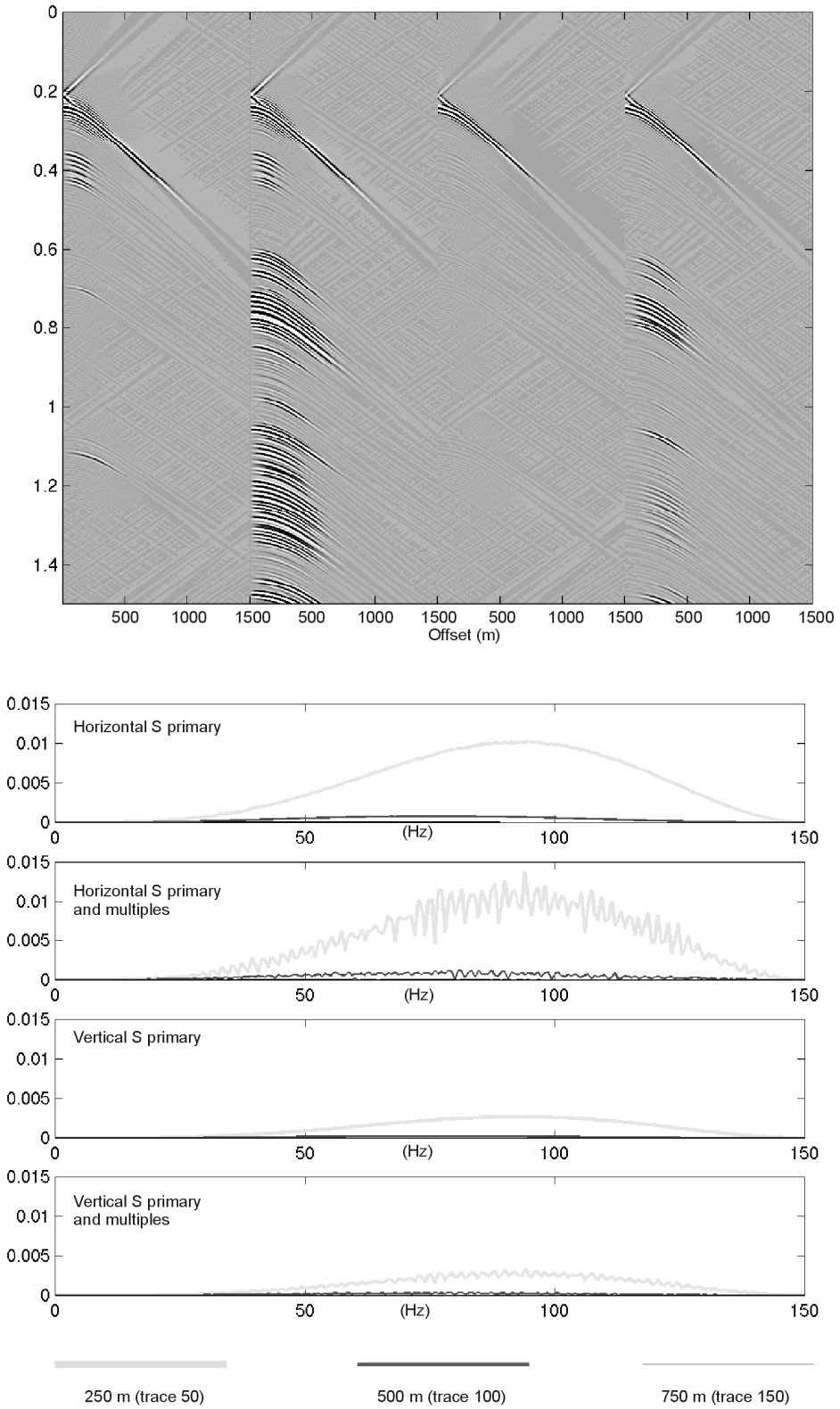

Figure. 7 The displacement fields and their amplitude spectral variation with offset for model II, in response of converted SV wave.

Contents

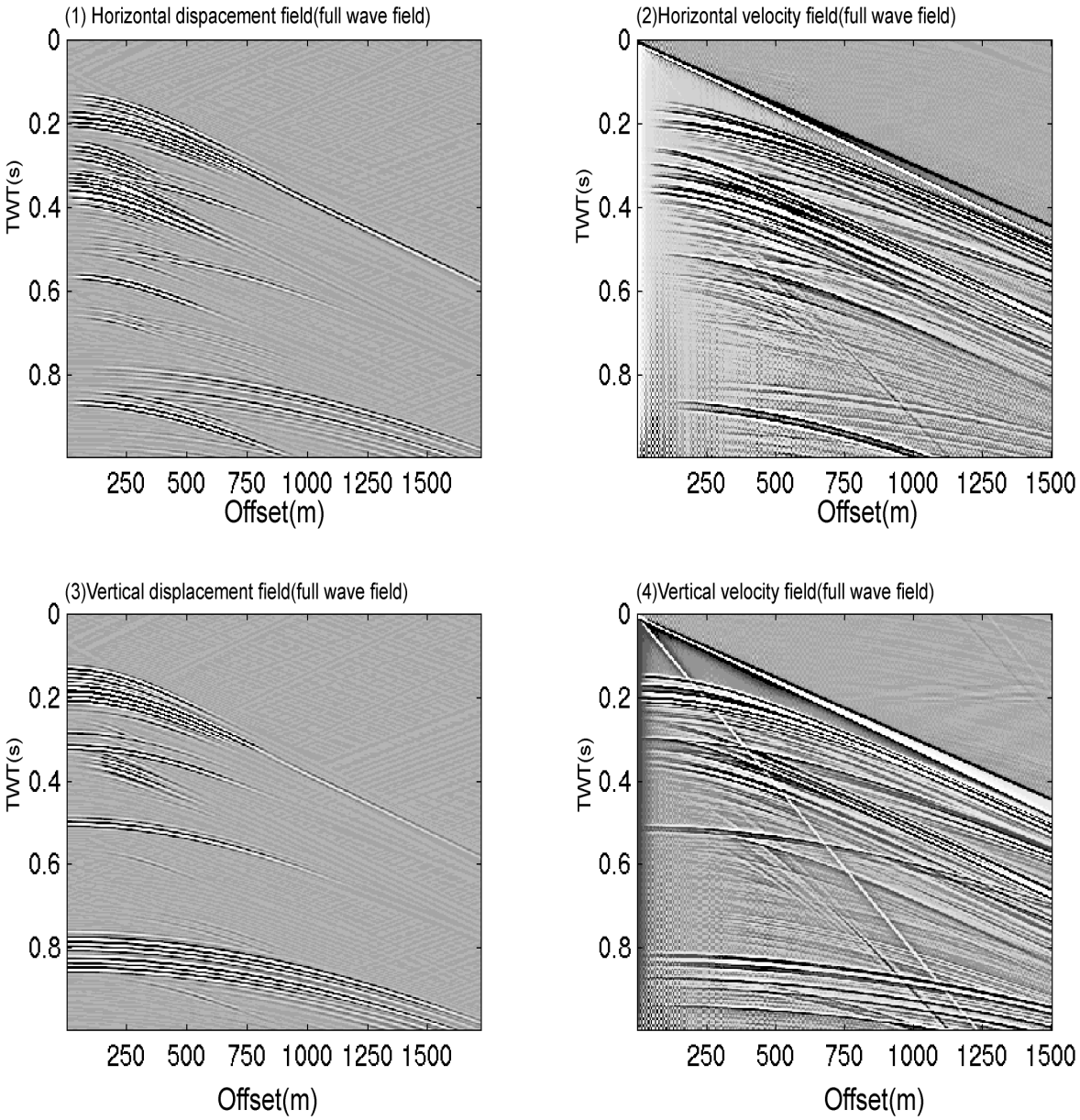

Figure. 8 The displacement fields in response of P and converted SV wave (ELMO) have rather similar feature with the velocity fields (OSIRIS) in term of P and SV primaries. However, OSIRIS generated stronger interbed P and SV multiples. However, note that the event group below 0.8 s seems to have more interbed multiples than that from OSIRIS. Also note that this event group is very weak near zero offset in OSIRIS data.

OSIRIS uses the global matrix method, which belongs to the approach of a continuous wave system in the frequency domain. The continuous wave system introduces several limitations to the type of problems that can be handled. Typically, the geometry has to be parallel or curved layers. Its frequency domain approach involves complicated computation details while its time domain approach is a

generalized ray summation. With the above limitations, OSIRIS is suitable for both horizontal and vertical spread (VSP) but not for complicated structures. However, there are several source representations in OSIRIS including shear wave source.

Numerical artifacts are present in both ELMO and OSIRIS. In ELMO, when the number of layers become larger and larger, steeply dipping artifacts get more and more dominant and finally the signal bandwidth become invisible. This happened when we tried to calculate the vertical primary with multiple displacement fields for the 102-layer model. In OSIRIS, the zero offset traces appear to have extremely large amplitude, however, the abnormal amplitude decreases quickly with offset to acceptable levels. The same effect seems to happen in the 24-layers model blocked from the whole well log.

Artifacts caused by wavefield wrap-around are related to the finite extent of the model and occurs in both ELMO and OSIRIS. This artifact is expressed as the dipping straight lines in the synthetic data. They are actually the wrap-around in the in the inverse Fourier transform. Their effect on the synthetic data is not serious when the number of layers is small, but tremendous when the number of layers get as large as 102 layers, which makes some of the calculated wavefields uninterpretable. However, efforts can be taken to reduce the artifacts, as discussed by Youzwishan and Margrave, 1998.

In term of calculation speed, OSIRIS is much faster than ELMO. For example, the calculation of P primary and multiples displacement fields for the 25-layer model, took ELMO about 1.5 hours to complete while it was only a matter of several minutes for OSIRIS. We believe this is mainly due to the fact that ELMO is an unoptimized research code running in Matlab. Algorithm efficiency could be a factor, however, we are sure it is not dominant.

DISCUSSION AND CONCLUSIONS

Several studies of multiple scattering effect have been done using models with a stack of thin sediment layers between two homogeneous half space (for example, Shapiro et al, 1994). The model we used is based on realistic seismic survey geometry. The reflectivity received at surface is equivalent to the transmissivity across twice the number of layers. This indicates that reflectivity in a two-way travel path and transmissivity through a one-way travel path are directly comparable.

However, at present stage, we can not give a theoretical expression of the O'Doherty-Ansty formula specially for reflectivity attenuation. We can only compare our numerical result with the existing results and tell the possible trends. Amplitude spectrum variation with offset is clearly observed in the P wave primary data calculated with ELMO, possibly this is due to the increment of transmission loss with offset.

The multiple scattering effect variation with the thickness of the layers or the number of layers within a certain depth interval was not clearly observed in the data calculated with ELMO. We can not compare our numerical result with others'

because we could not find any theoretical solution or numerical result previously done on this topic. This can be a possible future research topic.

The displacement (P primary) and velocity (full wavefield) amplitude variation with offset was clearly observed in both ELMO and OSIRIS data. However, they seem to have opposite variation trend, i.e., that of 25-layer remain strongest in the primary displacement field while its velocity spectrum remains minimal in the three thin layer models. The difference between the variation trends may indicates possible effects of multiple scattering. However, there is some coherency between them as we observed that both the displacement and velocity field spectrum are rather close to each other for the 57- and 102-layer models. Possibly, there is a threshold value for the number of layers, at which the multiple effect will change rather fast. This threshold value may also have some relation with the frequency content of the input wavelet. This may require more work in examining both the modeling theory and computing algorithm to understand the difference.

FUTURE WORK

Besides the possible future work mentioned above, there is much more work to do with this interesting topic. The effect of multiple scattering on both PP and PS wavefield, besides its offset/angle dependency, should also have certain relation with the geological complexity. Theoretical research work can be very challenging. As often found in the overburden of many reservoirs, fine sand/shale layers are geological realization of the fine-layer models. The effect on the reflection below, such as oil/water contact, is crucial in amplitude versus offset (AVO) analysis. It is a big challenge to develop theory and practical ways of multiple scattering effect corrections for AVO analysis.

REFERENCE

Banik, N.C., Lerche, I., and Shuey, R.T., 1985, Stratigraphic filtering, part I: Derivation of the O'doherty-Ansty formula, Geophysics, 50,2768-2744.

O'doherty, R. F. and Ansty, N.A., 1971, Reflection on amplitudes. Geophysical Prospecting, 19, 430-458

Serge A. Shapiro, Holger Zient and Peter Hubrual, 1994, A generalized O'Doherty-Ansty formula for waves in finely layered media, Geophysics. 59, 1750-1762.

Serge A. Shapiro and Peter Hubral, 1996, Elastic waves in finely layered sediments: The equivalent medium and generalized O'Doherty-Ansty formulas, Geophysics. 61, 1282-1300.

Silawongsawat, C., 1998, Elastic wavefield modeling by phase shift cascade, M.Sc. thesis, Department of Geology and Geophysics, University of Calgary.

Silawonsawat, C., and Margrave, G. F., 1997, Elastic wavefield modeling by phase shift cascade, CREWES Project Annual Report, 13.

Schmidt, H & Tango., 1986, Efficient global matrix approach to the computation of synthetic seismograms, Geophysical Journal of the Royal Astronomic Society, 84, pp 331-359.

Vilmann, O., Gerstoft, P. and Krenk, S., 1989, High speed forward modeling applied in seismic data processing, Ødegaard A/S, Report 89.238.

Widmaier, M., Muller, T., Shapiro, S.A., and Hubral, P., 1995, Amplitude preserving migration and elastic P-wave AVO corrected for thin layering, Journal of Seismic Exploration, 4, 169-177.

Youzwishan, C., Margrave, G.F., 1998, User's guide to the elastic wavefield modeling with ELMO software package, CREWES Annual Report, 1998.